© 2014. Published by The Company of Biologists Ltd | Development (2014) 141, 2691-2701 doi:10.1242/dev.108944

RESEARCH ARTICLE

# FGF signaling activates a Sox9-Sox10 pathway for the formation and branching morphogenesis of mouse ocular glands

**Ziyan Chen[1,2,*], Jie Huang[2,*], Ying Liu[2], Lisa K. Dattilo[2], Sung-Ho Huh[3], David Ornitz[3] and David C. Beebe[2,4,‡]**

## ABSTRACT

Murine lacrimal, harderian and meibomian glands develop from the prospective conjunctival and eyelid epithelia and produce secretions that lubricate and protect the ocular surface. Sox9 expression localizes to the presumptive conjunctival epithelium as early as E11.5 and is detected in the lacrimal and harderian glands as they form. Conditional deletion showed that *Sox9* is required for the development of the lacrimal and harderian glands and contributes to the formation of the meibomian glands. Sox9 regulates the expression of Sox10 to promote the formation of secretory acinar lobes in the lacrimal gland. Sox9 and FGF signaling were required for the expression of cartilage-associated extracellular matrix components during early stage lacrimal gland development. *Fgfr2* deletion in the ocular surface epithelium reduced Sox9 and eliminated Sox10 expression. *Sox9* deletion from the ectoderm did not affect *Fgf10* expression in the adjacent mesenchyme or *Fgfr2* expression in the epithelium, but appeared to reduce FGF signaling. *Sox9* heterozygotes showed a haploinsufficient phenotype, in which the exorbital branch of the lacrimal gland was absent in most cases. However, enhancement of epithelial FGF signaling by expression of a constitutively active FGF receptor only partially rescued the lacrimal gland defects in *Sox9* heterozygotes, suggesting a crucial role of Sox9, downstream of FGF signaling, in regulating lacrimal gland branching and differentiation.

**KEY WORDS: Sox9, Sox10, FGF signaling, Lacrimal gland, Harderian gland**

## INTRODUCTION

The formation of ocular glands is a key process during ocular surface development. Murine lacrimal, harderian and meibomian glands and goblet cells develop from the prospective conjunctival and eyelid epithelia and produce secretions that lubricate and protect the ocular surface. Ocular gland morphogenesis involves epithelial specification, bud outgrowth, branching and acinar differentiation.

Fibroblast growth factor (FGF) signaling is required for the formation of the lacrimal and harderian glands. Lacrimal and harderian gland development begins on embryonic day (E) 13.5 and 15.5, respectively, when Fgf10 in the periocular mesenchyme interacts with fibroblast growth factor receptor 2b (Fgfr2b) in the ectoderm to induce bud outgrowth (Govindarajan et al., 2000; Makarenkova et al., 2000; Tsau et al., 2011; Qu et al., 2012). Components of the extracellular matrix (ECM) are required to enhance FGF signaling during lacrimal gland induction, including heparan sulfate-containing glycosaminoglycans (GAGs). Negatively charged GAGs control the FGF-FGFR interaction to activate downstream signaling, limit the diffusion of Fgf10 and stabilize the FGFs in the mesenchyme (Qu et al., 2012). Inactivation of heparan sulfate biosynthesis enzymes in the prospective lacrimal gland epithelium prevents the formation of lacrimal glands; the lacrimal gland was either severely reduced in size or missing in *Ndst1* mutants and lost altogether in *Ndst1/2* double mutants (Pan et al., 2008). *Hs2st; Hs6st* double mutants also lacked lacrimal gland development (Qu et al., 2011). In *Ugdh* mutants, loss of GAGs resulted in excessive Fgf10 diffusion, which inhibited lacrimal gland budding (Qu et al., 2012).

Other factors involved in lacrimal gland formation include the transcription factor Pax6, which is required in the conjunctival epithelium for the outgrowth of the lacrimal bud (Makarenkova et al., 2000). Small eye (Sey) mice with a mutation in one copy of *Pax6* have vestigial lacrimal glands (Makarenkova et al., 2000). Barx2 and Fgf10 regulate ocular gland branching morphogenesis by controlling the expression of matrix metalloproteinases (MMPs) and epithelial cell migration through the ECM (Tsau et al., 2011). Bmp7 is required for the formation of mesenchymal condensations and branching of the lacrimal gland (Dean et al., 2004). Foxc1 mediates the BMP signaling required for lacrimal gland development (Mattiske et al., 2006). *Klf5* conditional null lacrimal glands showed a disrupted acinar organization (Kenchegowda et al., 2011) and *Six1*$^{-/-}$ fetuses displayed small lacrimal glands (Laclef et al., 2003). However, little is known about the mechanisms required to initiate lacrimal gland formation by FGF signaling.

To address this question, we used microarray analysis to identify differentially expressed genes in the murine presumptive corneal, conjunctival and eyelid epithelium at E12.5. We found that Sox9 was preferentially expressed in presumptive conjunctival epithelium. This prompted us to investigate the function of Sox9 in the developing ocular surface epithelium. Using conditional deletion and a second microarray analysis, we found that Sox9 regulates the expression of Sox10. *Sox9* and *Sox10* conditional knockouts were used to investigate how these transcription factors contribute to the development of the lacrimal and harderian glands.

## RESULTS

### Sox9 is expressed in the developing ocular glands

To investigate the role of Sox9 during embryonic ocular surface development, we examined the stage- and cell-specific distribution of Sox9 (Fig. 1A-L). Sox9 protein was initially detected in cell nuclei scattered throughout the ocular surface epithelium at E10.0-11.5. At E10.0-10.5, nuclear Sox9 expression was found in some lens pit cells, but was not detectable in the lens after E11.5 (Fig. 1A-C, arrows). By E12.5, Sox9 preferentially localized to the prospective conjunctival epithelium (Fig. 1D, arrow). Sox9 could also be detected in the retina,

[1]State Key Laboratory of Ophthalmology, Zhongshan Ophthalmic Center, Sun Yat-sen University, Guangzhou 510060, China. [2]Department of Ophthalmology and Visual Sciences, Washington University, St Louis, MO 63130, USA. [3]Department of Developmental Biology, Washington University, St Louis, MO 63130, USA. [4]Department of Cell Biology and Physiology, Washington University, St Louis, MO 63130, USA.
*These authors contributed equally to this work

‡Author for correspondence (beebe@wustl.edu)

**Received 11 February 2014; Accepted 6 May 2014**

Development (2014) 141, 2691-2701 doi:10.1242/dev.108944

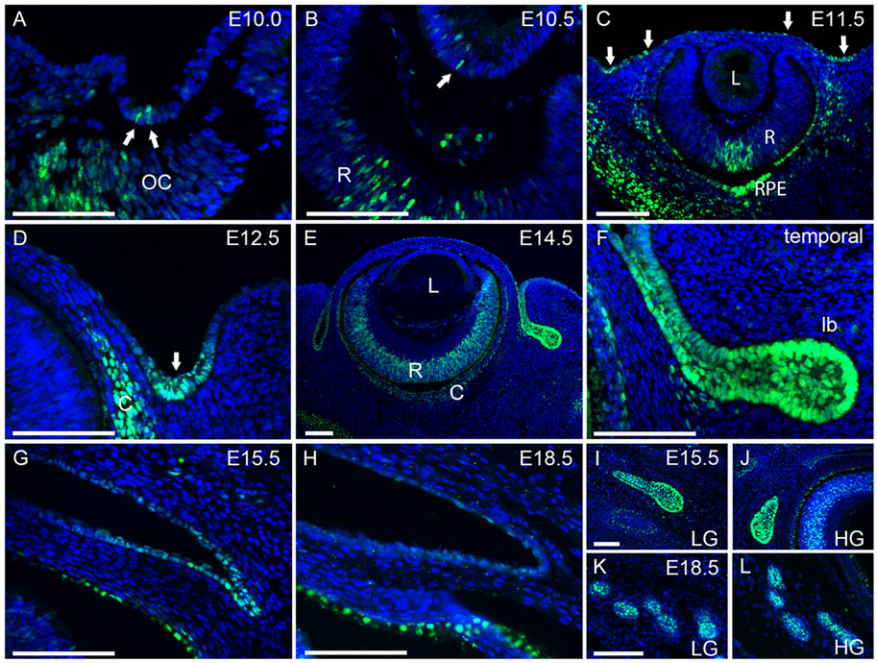


**Fig. 1. Sox9 expression during development of the ocular surface epithelia.** (A-C) Sox9 expression was first visible in a few lens pit cells at E10.0-10.5 (A,B, arrows). Expression ceased in the lens and spread throughout the ocular surface epithelium at E11.5, with evidence of concentration in the future conjunctival region (C, arrows). (D-F) Sox9 expression became restricted to the prospective conjunctival epithelium at E12.5 (D, arrow) and was expressed in the primary lacrimal bud epithelium at E14.5 (E,F). (G-L) Sox9 expression decreased in the conjunctival epithelium after E15.5 (G) and was hardly detected at E18.5 (H). However, Sox9 continued to be abundantly expressed in the epithelium of the lacrimal and harderian glands (I-L). lb, lacrimal bud; LG, lacrimal gland; HG, harderian gland; OC, optic cup; R, retina; L, lens; C, choroid; RPE, retinal pigmented epithelium. Scale bars: 100 μm.

retinal pigmented epithelium and the choroid. The murine lacrimal gland begins to form at E13.5 as a projection from the temporal conjunctival epithelium into the surrounding mesenchyme, and the harderian glands originate by a similar process from the nasal part of the conjunctival epithelium at E15.5 (Tsau et al., 2011). At E14.5, Sox9 was expressed in the nuclei of conjunctival and primary lacrimal bud epithelial cells (Fig. 1E,F). Sox9 expression decreased in the conjunctival epithelium after E15.5 (Fig. 1G), becoming undetectable at birth (Fig. 1H). However, Sox9 expression remained in the epithelium of the lacrimal and harderian glands (Fig. 1I-L).

## Sox9 is required for the development of the lacrimal gland

In order to determine how Sox9 might influence ocular surface development, we used the *Le-Cre* transgene to delete floxed

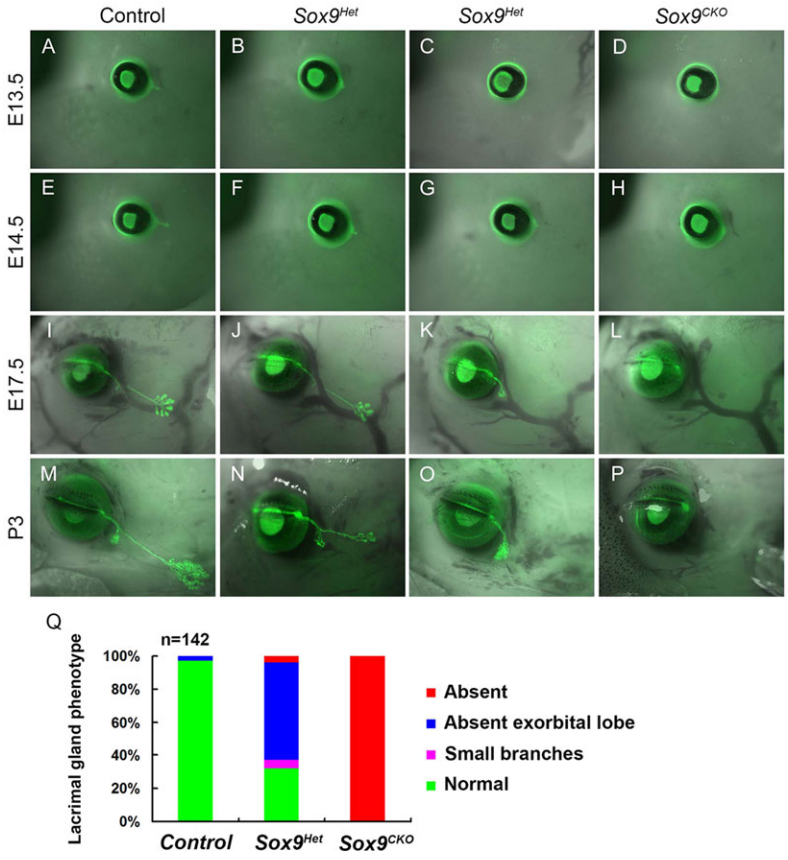


**Fig. 2. *Sox9* is required for the development of the lacrimal gland.** (A-H) Lacrimal gland phenotypes were visualized by GFP expression from the *Le-Cre* transgene. The primary lacrimal bud formed at E13.5 and elongated at E14.5 (A,E). By contrast, lacrimal buds of $Sox9^{Het}$ embryos showed delayed budding and extension (B,C,F,G) and $Sox9^{CKO}$ embryos showed no bud formation (D,H). (I-P) Between E17.5 and P3, the intraorbital and exorbital lobes of the lacrimal glands formed and branched extensively in wild-type mice (I,M), whereas $Sox9^{Het}$ lacrimal glands were poorly branched (J,N) and, in some cases, lacked exorbital lobes (K,O), and $Sox9^{CKO}$ animals failed to develop lacrimal glands (L,P). (Q) Summary of lacrimal gland phenotypes in wild-type, $Sox9^{Het}$ and $Sox9^{CKO}$ P3 newborns ($n$=142 lacrimal glands). $Sox9^{+/+}$; $Le\text{-}Cre^{+/-}$ embryos were used as controls.

Development (2014) 141, 2691-2701 doi:10.1242/dev.108944

alleles of *Sox9* in the ocular surface (Akiyama et al., 2002). The *Le-Cre* transgene, which carries a *Cre-IRES-GFP* cassette, targets the lens and the ocular surface epithelia, including the epidermis of the eyelid, and the corneal, conjunctival, lacrimal and meibomian gland epithelia (Ashery-Padan et al., 2000). The phenotype of the lacrimal glands in *Sox9* mutant mice could be observed by the expression of the *Le-Cre* GFP reporter (Fig. 2A-P). $Sox9^{+/+}$; $Le\text{-}Cre^{+}$ mice were used as controls, in which the GFP labeled the developing lacrimal gland.

In $Sox9^{flox/flox}$; $Le\text{-}Cre^{+}$ (referred to as $Sox9^{CKO}$) mice, the lacrimal buds were absent at E13.5 (Fig. 2D), which is the stage when they form in the control mice (Fig. 2A). No lacrimal glands were present in $Sox9^{CKO}$ mice at birth (Fig. 2H,L,P). Mice heterozygous for *Sox9* had variable degrees of defective lacrimal gland morphogenesis (Fig. 2B,C,F,G,J,K,N,O). $Sox9^{flox/+}$; $Le\text{-}Cre^{+}$ (referred to as $Sox9^{Het}$) mice showed delayed budding and bud elongation at E13.5 and E14.5 (Fig. 2B,C,F,G) relative to the control mice (Fig. 2A,E). In wild-type mice, after the extension of the lacrimal bud, the intraorbital lobe of the gland forms by E17.5, while the exorbital lobe continues extension and branching (Fig. 2I,M). *Sox9* heterozygotes had either vestigial exorbital lobes (Fig. 2K,O) or small branches (Fig. 2J,N). At postnatal day (P) 3, when both intraorbital and exorbital lobes branched extensively in wild-type mice (Fig. 2M), the single vestigial exorbital lobe in $Sox9^{Het}$ mice continued to branch slightly, although there was no evidence of lacrimal duct extension (Fig. 2O).

Owing to the variation in lacrimal gland phenotypes of $Sox9^{Het}$ mice, we examined 142 glands of P3 animals (Fig. 2Q): in the control $Le\text{-}Cre^{+}$ pups, only 3% had vestigial exorbital lobes; 100% of $Sox9^{CKO}$ pups lacked lacrimal glands; 58.7% of $Sox9^{Het}$ animals had one vestigial lobe, 32% had normal gland structures, 5.3% had small branches and 4% had no lacrimal glands.

### Sox9 is required for the development of the harderian gland and contributes to the formation of the meibomian glands

Sox9 was expressed in the harderian gland epithelium. Hematoxylin and Eosin (H&E) staining of serial sections showed that the epithelial component of harderian glands was absent in P3 $Sox9^{CKO}$ mice, although the mesenchyme in which the gland would have formed was present (Fig. 3C, arrow). The gland structure in $Sox9^{Het}$ mice (Fig. 3B, arrow) appeared similar to wild type (Fig. 3A, arrow). We also examined whether loss of *Sox9* affected the formation of the meibomian glands. One-month-old wild-type upper and lower eyelids showed meibomian glands with well-branched acinar structures (Fig. 3D). By contrast, $Sox9^{CKO}$ mice had ~40% fewer glands in the upper and lower eyelids ($P<10^{-5}$ for each) and most glands had fewer acini (Fig. 3E).

Although Sox9 was abundant in the conjunctival epithelium at E12.5-14.5, the formation of eyelids and conjunctival epithelium appeared normal in $Sox9^{CKO}$ mice (Fig. 3H-K). $Sox9^{CKO}$ mice had normal eyelid growth, closure and reopening during embryonic and postnatal development (data not shown). Fluorescent *in situ* hybridization (FISH) showed normal expression of keratin 4 (*Krt4*) mRNA, a conjunctival epithelium differentiation marker, in P3 $Sox9^{CKO}$ mice (Fig. 3H,I, arrowheads). The formation of conjunctival goblet cells, which produce mucus to lubricate the ocular surface, was unaffected in adult $Sox9^{CKO}$ mice (Fig. 3J,K, arrows). Since Sox9 is a regulator of hair follicle differentiation and stem cells (Vidal et al., 2005), *Sox9* deletion was associated with missing hair in the mouse eyelids and facial skin (Fig. 3G).

### Sox9 regulates the expression of Sox10 to promote branching and the formation of secretory acini in the lacrimal gland

To investigate the molecular mechanisms by which Sox9 regulates lacrimal gland formation, we laser microdissected the dorsal, nasal and temporal regions of the conjunctival epithelium

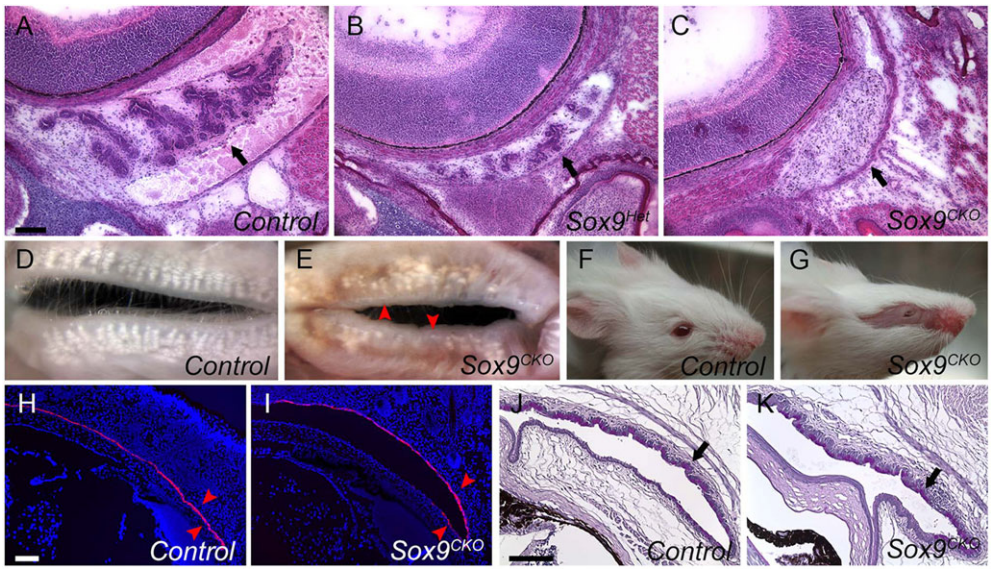


**Fig. 3. Harderian and meibomian gland phenotypes and normal conjunctiva formation in $Sox9^{CKO}$ mice.** (A-C) H&E staining of selected serial sections of the harderian gland at P3 showed that the harderian gland epithelium was present in wild type (A, arrow), reduced in $Sox9^{Het}$ mice (B, arrow) and absent in $Sox9^{CKO}$ mice, although the mesenchyme remained (C, arrow). (D,E) View of the inner surface of eyelids from adult wild-type (D) and $Sox9^{CKO}$ (E) mice showing reduced numbers of meibomian glands in both eyelids in the *Sox9* mutant mice. (F,G) A $Sox9^{CKO}$ mouse at 3 weeks of age showing absence of hair on the eyelids and facial skin where the *Le-Cre* transgene was expressed. (H,I) Fluorescent RNA *in situ* hybridization (FISH) for keratin 4 (*Krt4*) in conjunctival epithelium from wild-type (H) and $Sox9^{CKO}$ (I) animals at P3. *Krt4* expression in $Sox9^{CKO}$ pups (I, arrowheads) was similar to that in wild type (H, arrowheads). (J,K) Normal PAS staining pattern for conjunctiva goblet cells (arrow) in 3-month-old $Sox9^{CKO}$ mice (K) relative to the wild-type mice (J). Scale bars: 100 μm.

Development (2014) 141, 2691-2701 doi:10.1242/dev.108944

**Table 1. Microarray analysis of gene expression comparing E14.5 *Sox9* null temporal conjunctival epithelium with wild type**

| Gene | Fold change |
|---|---|
| *Sox10* | –5.3 |
| *Mia1* | –4.6 |
| *Col2a1* | –12.0 |
| *Col9a1* | –9.8 |
| *Col9a2* | –2.5 |
| *Col9a3* | –2.1 |
| *Hs3st3b1* | –5.9 |
| *Hs3st3a1* | –2.5 |
| *Etv5* | –2.3 |
| *Dusp6* | –2.3 |

Transcripts encoding Sox10, melanoma inhibitory activity 1 (Mia1), the cartilage-associated ECM components collagen type II (Col2a1) and collagen type IX (Col9a1, Col9a2, Col9a3), the FGF signaling-associated factors heparan sulfate 3-O-sulfotransferase 3B1 and 3A1 (Hs3st3b1 and Hs3st3a1), ets variant gene 5 (Etv5) and dual specificity phosphatase 6 (Dusp6) were reduced in expression by at least 2-fold in E14.5 $Sox9^{flox/flox}$; $Le\text{-}Cre^{+}$ temporal conjunctival epithelium compared with wild-type embryos.

in E14.5 $Sox9^{CKO}$ and wild-type embryos to perform microarray analysis. Gene expression was compared in the temporal conjunctival epithelium, where the primary lacrimal bud forms. *Sox10* transcripts were decreased greater than 5-fold, compared with wild type (Table 1). Immunostaining showed that Sox10 was expressed primarily in the bud tip cells at E13.5 (Fig. 4A, dotted line). Sox10 protein was not detectable in presumptive bud epithelium in $Sox9^{CKO}$ embryos (Fig. 4B, dotted line). Quantitative PCR (qPCR) confirmed that the transcript level for *Sox10* was substantially decreased in $Sox9^{CKO}$ temporal conjunctival epithelium (Fig. 4E).

To determine whether *Sox10* is important for the development of the lacrimal gland, *Le-Cre* mice were crossed with mice carrying $Sox10^{flox}$ alleles (Finzsch et al., 2010). Mice heterozygous for *Sox10* (referred to as $Sox10^{Het}$) showed the normal pattern of lacrimal gland development (Fig. 5A,C,E). At E14.5, the primary lacrimal bud was present, but shorter in $Sox10^{flox/flox}$; $Le\text{-}Cre^{+}$ (referred to as $Sox10^{CKO}$) embryos than in wild type (Fig. 5B, arrow). Sox9 expression remained in the epithelium of the short bud in $Sox10^{CKO}$ mice (Fig. 4D, arrow), confirming that Sox10 is downstream of Sox9 during lacrimal gland formation. By E17.5, the lacrimal gland in $Sox10^{CKO}$ embryos was small and poorly branched (Fig. 5D). $Sox10^{CKO}$ mice showed minimal branching at P3 (Fig. 5F, arrow). H&E staining provided no evidence of secretory acini in P3 $Sox10^{CKO}$ lacrimal (Fig. 5H) or harderian (Fig. 5J) glands. These data show that Sox10 is regulated by Sox9 and is necessary for lacrimal gland branching and acini formation.

### Sox9 regulates the expression of cartilage-associated factors during early stage lacrimal gland development

From the microarray data, we also found that cartilage-associated factors were decreased in $Sox9^{CKO}$ mice. These genes, which showed a greater than 2-fold decrease in expression in *Sox9*-deleted temporal conjunctival epithelium, included melanoma inhibitory activity 1 [*Mia1*; also known as *Mia* or cartilage-derived/retinoic acid-sensitive protein (*Cdrap*)] and genes encoding the cartilage ECM proteins collagen II and collagen IX (Table 1).

Mia1 stabilizes cartilage differentiation and inhibits cartilage differentiation into bone (Schubert et al., 2010). Sox9 regulates Mia1 expression through binding to a SOX consensus sequence in the *Mia1* promoter (Xie et al., 1999). Mia1 is also an FGF-regulated protein during lung branching morphogenesis (Lin et al., 2008) and is decreased in expression in the *Sox9* mutant lung (Chang et al., 2013). Our data showed that *Mia1* mRNA was strongly expressed in primary lacrimal bud tip cells at E13.5 (Fig. 6A, dotted line), whereas it was not detectable in the presumptive bud epithelium of the $Sox9^{CKO}$ embryo (Fig. 6B, dotted line). $Sox10^{CKO}$ mice had shorter buds, which still expressed *Mia1* (Fig. 6C, dotted line).

Collagens II and IX are the primary collagens found in cartilage matrix and Sox9 promotes *Col2a1* gene expression during chondrogenesis (Bridgewater et al., 1998). Sox9 also regulates Col2a1 expression during lung development (Rockich et al., 2013). Col2a1 protein was expressed in the ECM surrounding the conjunctival and lacrimal bud epithelium (Fig. 6E, arrow) but away from the bud tip (Fig. 6E, arrowhead). By contrast, Col9a1 protein appeared to be secreted from the apical bud tip cells (Fig. 6I, arrow). The expression of Col2a1 and Col9a1 was undetectable in $Sox9^{CKO}$ temporal conjunctival epithelium (Fig. 6F,J, dotted line, arrow). However, the expression of these collagens remained in the $Sox10^{CKO}$ mice (Fig. 6G,K, arrow). Reduced expression of *Mia1*, *Etv5* and *Col2a1* was detected in $Sox9^{Het}$ lacrimal glands (supplementary material Fig. S1).

### Sox9-regulated transcripts appear to be co-regulated by FGF signaling

Fgf10 is an inductive signal for the lacrimal and harderian glands (Makarenkova et al., 2000). Fgf10 expressed at the temporal and nasal sides of the periocular mesenchyme acts directly on the conjunctival epithelium to stimulate primary bud formation and proliferation of cells within the bud. However, Fgf10 is expressed at low levels in the dorsal and ventral mesenchyme, and the dorsal conjunctival epithelium is unresponsive to Fgf10 in producing an ectopic lacrimal bud (Makarenkova et al., 2000). We compared gene expression in wild-type dorsal and temporal conjunctival epithelium and found that Sox9-regulated transcripts were preferentially

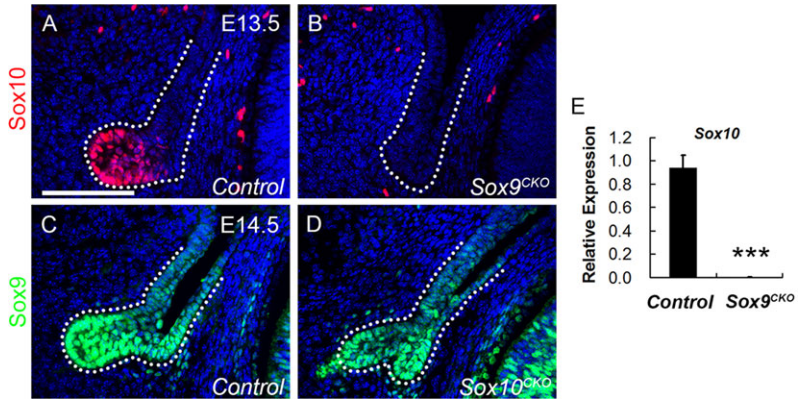


**Fig. 4. *Sox9* is required for the expression of *Sox10* during lacrimal gland formation.** (A,B) Deletion of *Sox9* resulted in the loss of *Sox10* staining in the presumptive bud epithelium at E13.5 (dotted line). (C,D) *Sox10* deletion maintained *Sox9* expression in the poorly developed bud epithelium at E14.5 (dotted line). (E) qPCR analysis of relative *Sox10* mRNA expression in E14.5 wild-type (control) and $Sox9^{CKO}$ temporal conjunctival epithelium. $n$=3; ***$P$<0.0001, Student's $t$-test; error bars represent s.d. Scale bar: 100 μm.

Development (2014) 141, 2691-2701 doi:10.1242/dev.108944

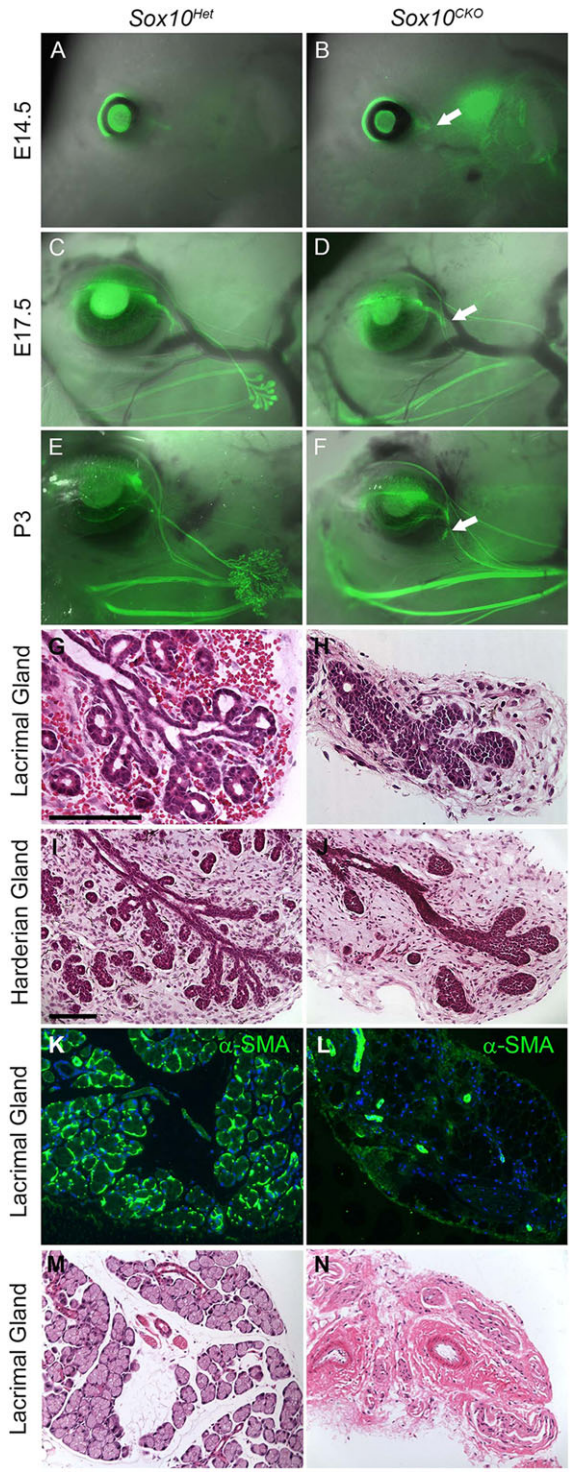


**Fig. 5. *Sox10* is required for the formation of secretory acini in lacrimal and harderian glands.** (A-F) Lacrimal gland phenotypes in $Sox10^{Het}$ and $Sox10^{CKO}$ mice. At E14.5, the primary lacrimal bud was present but shorter in $Sox10^{CKO}$ embryos (B, arrow). $Sox10^{CKO}$ glands had short, poorly branched lacrimal ducts at E17.5 (D, arrow) and P3 (F, arrow). (G-J) No evidence of secretory acini was detected in $Sox10^{CKO}$ lacrimal (H) or harderian (J) glands compared with wild type at P3 (G,I). (K,L) $Sox10^{Het}$ lacrimal glands at P21 had numerous myoepithelial cells stained for α-smooth muscle actin surrounding clusters of acinar cells. No myoepithelial cells were detectable in the $Sox10^{CKO}$ glands – just a few medium-size blood vessels. (M,N) H&E staining showed clusters of acini in P21 $Sox10^{Het}$ lacrimal glands, whereas $Sox10^{CKO}$ glands had no apparent acini – only blood vessels and what appeared to be degenerated ducts. Scale bars: 100 μm.

expressed in the temporal domain, including *Sox10*, *Mia1*, *Col2a1* and *Col9a1* (data not shown). We then performed microarray analysis to examine gene expression in $Fgfr2^{flox/flox}$; *Le-Cre* (referred to as $Fgfr2^{CKO}$) and wild-type temporal conjunctival epithelium. These Sox9-regulated transcripts were found to be significantly decreased after deletion of *Fgfr2*. FISH and antibody staining confirmed that the expression of Sox10, *Mia1*, Col2a1 and Col9a1 was undetectable in $Fgfr2^{CKO}$ mice (Fig. 6D,H,L and Fig. 7D). qPCR also showed that the transcript level for *Sox10* diminished significantly in $Fgfr2^{CKO}$ temporal conjunctival epithelium (Fig. 7E).

### *Fgfr2* deletion reduces Sox9 expression and *Sox9* deletion reduces FGF signaling

Since Fgf10-Fgfr2 signaling is required for lacrimal gland formation, we tested the relationship between Sox9 and FGF signaling. First, we determined whether *Sox9* inactivation in the conjunctival epithelium affects the expression of *Fgf10* in the mesenchyme. At E13.5, $Sox9^{CKO}$ and $Sox10^{CKO}$ mice maintained similar expression of *Fgf10* mRNA to that of the control in the periocular mesenchyme surrounding the bud epithelium (Fig. 8A-C, dotted line). Despite the normal expression of *Fgf10* mRNA in the mesenchyme, our microarray analysis suggested reduced FGF signaling during lacrimal gland development (Fig. 8E,H,K,N, dotted line, 8P; Table 1).

Deletion of the heparan sulfate sulfotransferases *Hs2st* and *Hs6st* from the periocular mesenchyme increased the diffusion of Fgf10 in the ECM, decreased FGF signaling in the lacrimal gland bud and prevented lacrimal gland development (Qu et al., 2011). Heparan sulfate is required for the interaction of FGFs with FGF receptors (Qu et al., 2012). Heparan sulfate (glucosamine) 3-O-sulfotransferase 3B1 (*Hs3st3b1*) and 3A1 (*Hs3st3a1*) mRNA were strongly expressed in lacrimal bud tip cells (Fig. 8D,G, arrow, dotted line), but were not detected in the presumptive bud epithelium lacking *Sox9* (Fig. 8E,H, arrow, dotted line). However, in wild-type and $Sox9^{CKO}$ mice, *Hs3st3b1* and *Hs3st3a1* mRNAs were expressed at similar levels in the mesenchyme adjacent to the lacrimal gland bud, where *Fgf10* is expressed (Fig. 8D,E,G,H, dotted line). The transcript levels for *Hs3st3b1* and *Hs3st3a1* were examined by qPCR at E14.5 and were decreased in $Sox9^{CKO}$ temporal conjunctival epithelium (Fig. 8P).

ERK phosphorylation is one measure of FGF receptor activation. Activation of the MAP kinase pathway increases levels of the transcription factor Etv5, which promotes the expression of the dual-specificity phosphatase Dusp6, a feedback inhibitor of the MAP kinase pathway (Qu et al., 2012). Spry2 is also a feedback inhibitor expressed in response to FGF signaling (Pan et al., 2010). ERK phosphorylation and *Etv5*, *Dusp6* and *Spry2* expression were decreased in the presumptive lacrimal bud epithelium of $Sox9^{CKO}$ embryos at E14.5 (Table 1; Fig. 8K,N, dotted line, 8P). However, *Sox10* inactivation did not appear to affect these measures of FGF signaling. The expression of *Hs3st3b1*, *Hs3st3a1*, phospho-ERK and *Etv5* in $Sox10^{CKO}$ bud epithelium (Fig. 8F,I,L,O, dotted line) was similar to that in wild-type bud epithelium (Fig. 8D,G,J,M, dotted line). qPCR analysis of $Sox9^{CKO}$ epithelial cells indicated that *Hs3st3b1* and *Hs3st3a1* were significantly reduced, confirming the RNA FISH results. However, not all heparin-synthesizing enzymes were decreased (Fig. 8P). These results suggest that *Sox9* lacrimal gland defects might at least partially be caused by a Sox9-dependent reduction in FGF signaling.

### Activation of epithelial FGF signaling fails to rescue the lacrimal gland defects in *Sox9* heterozygotes

Since FGF signaling appeared to be reduced in $Sox9^{CKO}$ temporal conjunctival epithelium, we explored whether overexpression of

Development (2014) 141, 2691-2701 doi:10.1242/dev.108944

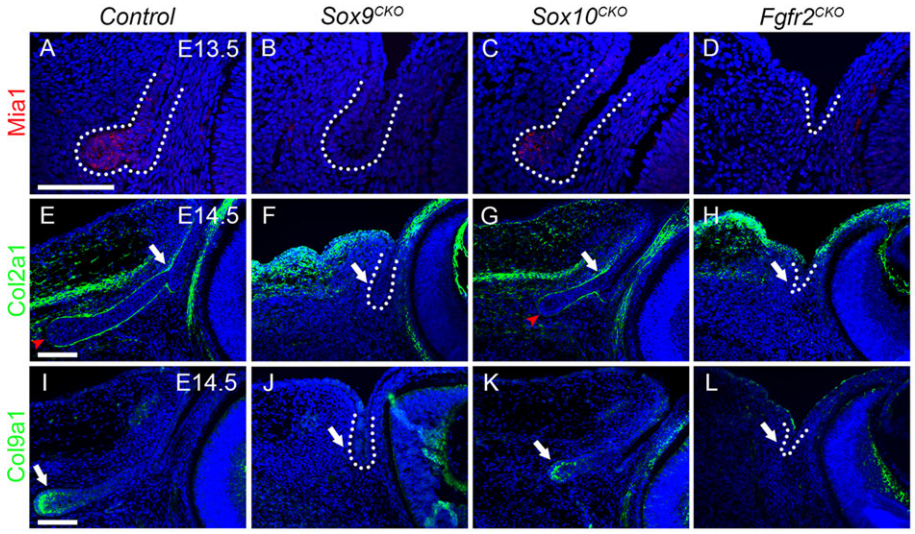


**Fig. 6. The expression of cartilage-associated factors in *Sox9*, *Sox10* and *Fgfr2* mutant early stage lacrimal glands.** (A-D) FISH for *Mia1* in wild-type (A), $Sox9^{CKO}$ (B), $Sox10^{CKO}$ (C) and $Fgfr2^{CKO}$ (D) embryos at E13.5. *Mia1* transcripts were detected in wild-type bud tip cells (A, dotted line), but not in presumptive bud epithelium after *Sox9* and *Fgfr2* deletion (B,D, dotted line) and were still present in $Sox10^{CKO}$ embryos (C, dotted line). (E-H) Immunostaining for Col2a1 in wild-type (E), $Sox9^{CKO}$ (F), $Sox10^{CKO}$ (G) and $Fgfr2^{CKO}$ (H) embryos at E14.5. Col2a1 surrounded the conjunctiva and lacrimal bud epithelium (E, arrow), except at the bud tip (E, arrowhead). Col2a1 expression was lost in $Sox9^{CKO}$ (F, dotted line, arrow) and $Fgfr2^{CKO}$ (H, dotted line, arrow) mutants but was maintained in the normal pattern in $Sox10^{CKO}$ buds (G, arrow, arrowhead). (I-L) Immunostaining for Col9a1 in wild-type (I), $Sox9^{CKO}$ (J), $Sox10^{CKO}$ (K) and $Fgfr2^{CKO}$ (L) embryos at E14.5. Col9a1 protein was mainly localized within and at the basal surface of the bud tip cells (I, arrow). Col9a1 expression was lost in $Sox9^{CKO}$ (J, dotted line, arrow) and $Fgfr2^{CKO}$ (L, dotted line, arrow) embryos but was present in $Sox10^{CKO}$ buds (K, arrow). Scale bars: 100 μm.

a constitutively active FGF receptor could rescue the lacrimal gland defects in *Sox9* heterozygotes. We crossed $Sox9^{CKO}$ animals with *TRE-Fgfr1; Rosa26-rtTA* mice, which produce a constitutively active form of Fgfr1. This construct contains a floxed STOP cassette in the *Rosa* locus upstream of the reverse tetracycline transactivator sequence. Cre-mediated recombination, driven by the *Le-Cre* transgene, would permit activation of FGF signaling by removing the STOP cassette (Belteki et al., 2005; Cilvik et al., 2013) while deleting the floxed *Sox9* allele. Mothers were fed doxycycline from E11.5 to create *Sox9* heterozygous embryos with activated FGF signaling. $Le\text{-}Cre^{+}$; $Sox9^{+/+}$; $TRE\text{-}Fgfr1^{+}$; $rtTA^{+}$ ($Sox9^{+/+}$; $TRE\text{-}Fgfr1^{+}$) mice were used as controls. These animals had lacrimal glands that appeared similar to those of $Le\text{-}Cre^{+}$; $Sox9^{+/+}$ mice, even though they were expected to have increased FGF signaling (data not shown). Lacrimal gland phenotypes were quantified in $Le\text{-}Cre^{+}$; $Sox9^{flox/+}$; $TRE\text{-}Fgfr1^{-}$; $rtTA^{+}$ ($Sox9^{Het}$; $TRE\text{-}Fgfr1^{-}$) and $Le\text{-}Cre^{+}$; $Sox9^{flox/+}$; $TRE\text{-}Fgfr1^{+}$; $rtTA^{+}$ ($Sox9^{Het}$; $TRE\text{-}Fgfr1^{+}$) pups at P3 (Table 2). $Sox9^{Het}$; $TRE\text{-}Fgfr1^{-}$ mice appeared similar to $Sox9^{Het}$ mice, with the majority lacking lacrimal glands or with the exorbital lobe absent. Although fewer $Sox9^{Het}$; $TRE\text{-}Fgfr1^{+}$ mice lacked lacrimal glands, a greater percentage lacked the exorbital lobe. These differences between $Sox9^{Het}$; $TRE\text{-}Fgfr1^{-}$ and $Sox9^{Het}$; $TRE\text{-}Fgfr1^{+}$ were statistically significant ($P$=0.004, Chi-square test). Thus, the expression of a constitutively active FGF receptor only marginally improves the *Sox9* haploinsufficiency phenotype.

To confirm the activation of FGF signaling in $Sox9^{Het}$; $TRE\text{-}Fgfr1^{+}$ mice, ERK phosphorylation was examined in E15.5 ocular epithelial cells (Fig. 9A-C). In control (wild-type) embryos, phosphorylation of ERK was apparent in the lacrimal bud tip (Fig. 9A, arrow) but was decreased in $Sox9^{Het}$; $TRE\text{-}Fgfr1^{-}$ mice (Fig. 9B, arrow). Phospho-ERK was not detectable in the palpebral conjunctiva in wild-type (Fig. 9A, arrowheads) or $Sox9^{Het}$; $TRE\text{-}Fgfr1^{-}$ (Fig. 9B, arrowheads) mice. In $Sox9^{Het}$; $TRE\text{-}Fgfr1^{+}$ mice, phospho-ERK was substantially increased in the epithelium of the lacrimal bud and palpebral conjunctiva (Fig. 9C, arrow and arrowheads), showing that FGF signaling was activated in these mice.

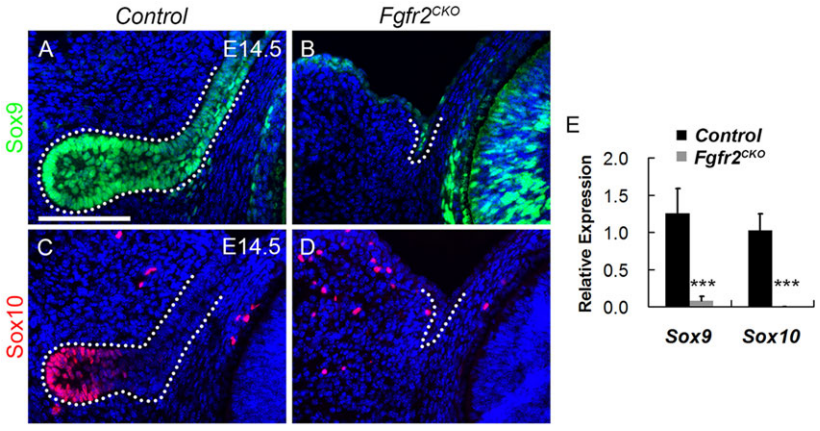


**Fig. 7. FGF signaling is required for the expression of Sox9 and Sox10.** (A,B) *Sox9* expression decreases in the temporal conjunctival epithelium in the $Fgfr2^{CKO}$ mutant (B, dotted line) compared with the wild type (A, dotted line). (C,D) The *Fgfr2* mutant showed no detectable Sox10 staining in the presumptive conjunctival epithelium (D, dotted line). (E) qPCR analysis of *Sox9* and *Sox10* expression in E14.5 temporal conjunctival epithelium, as normalized to *Actb* in $Fgfr2^{CKO}$ relative to the control mice. $n$=3; ***$P$<0.0001, Student's $t$-test; error bars represent s.d. Scale bar: 100 μm.

Development (2014) 141, 2691-2701 doi:10.1242/dev.108944

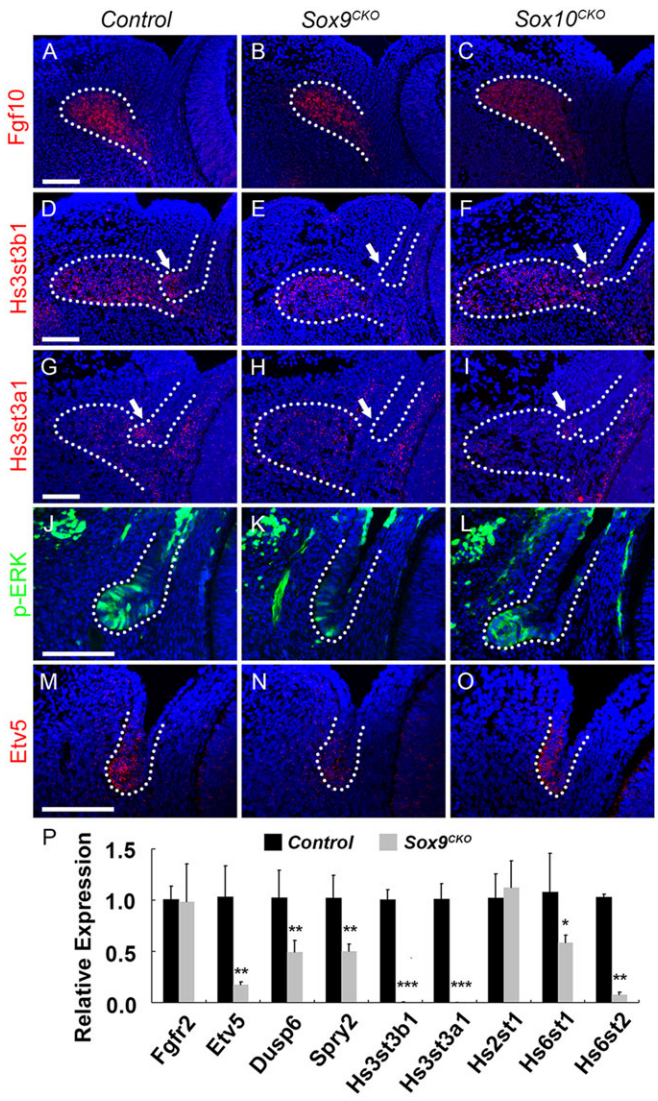


**Fig. 8. FGF signaling appears to be reduced after *Sox9* deletion.** (A-C) RNA FISH for *Fgf10* in periocular mesenchyme surrounding the lacrimal bud in E13.5 wild-type (A), $Sox9^{CKO}$ (B) and $Sox10^{CKO}$ (C) mice. Both $Sox9^{CKO}$ (B) and $Sox10^{CKO}$ (C) embryos had similar expression of *Fgf10* mRNA to the control (A). (D-I) RNA FISH for *Hs3st3b1* (D-F) and *Hs3st3a1* (G-I) in E14.5 wild-type (D,G), $Sox9^{CKO}$(E,H) and $Sox10^{CKO}$ (F,I) embryos. In wild-type mice, *Hs3st3b1* and *Hs3st3a1* mRNAs were detected both in lacrimal bud tip cells (D,G, arrow, dotted line) and the adjacent mesenchyme (D,G, dotted line). However, after *Sox9* deletion, *Hs3st3b1* and *Hs3st3a1* were expressed only in the adjacent mesenchyme (E,H, dotted line) but not in the presumptive bud epithelium (E,H, arrow, dotted line). *Sox10* deletion did not affect *Hs3st3b1* and *Hs3st3a1* expression in lacrimal bud tip cells (F,I, arrow, dotted line) or the adjacent mesenchyme (F,I, dotted line). (J-L) Immunostaining for phospho-ERK in wild-type (J), $Sox9^{CKO}$ (K) and $Sox10^{CKO}$ (L) mice. In wild-type mice, phospho-ERK was prominent in the invaginating bud epithelium (J). In $Sox9^{CKO}$ conjunctival epithelium, levels of phospho-ERK decreased markedly (K), whereas the $Sox10^{CKO}$ bud (L) exhibited a similar level of phospho-ERK to the wild-type bud epithelium (J). (M-O) RNA FISH for *Etv5* in E14.5 wild-type (M), $Sox9^{CKO}$ (N) and $Sox10^{CKO}$ (O) embryos. In wild-type mice, *Etv5* transcripts were readily detected in the primary bud epithelium (M). In $Sox9^{CKO}$ conjunctival epithelium, *Etv5* mRNA levels were greatly reduced (N); however, $Sox10^{CKO}$ buds expressed *Etv5* mRNA at a similar level to controls (O). (P) Transcripts for key members or targets of the FGF signaling pathways were quantified by qPCR analysis at E14.5 for control and $Sox9^{CKO}$ temporal conjunctival epithelium. There was no significant difference in the expression levels of *Fgfr2* between control and $Sox9^{CKO}$ epithelia. The transcript level for *Etv5*, *Dusp6* and *Spry2* decreased significantly in $Sox9^{CKO}$ embryos. *Hs3st3b1* and *Hs3st3a1* also showed a significant reduction, confirming the RNA FISH results. However, not all heparin-synthesizing enzymes were significantly decreased. $n$=3; *$P$<0.05, **$P$<0.001, ***$P$<0.0001, Student's $t$-test; error bars represent s.d. Scale bars: 100 μm.

## DISCUSSION

The SOX family is characterized by a high mobility group (HMG) DNA-binding domain with a high degree of homology to that of SRY (Pritchett et al., 2011). Sox9 belongs to SOX group E (SoxE), along with Sox8 and Sox10 (Foster et al., 1994). Sox9 has important functions in the development of several organs, including the liver, pancreas, lung and kidney (Furuyama et al., 2011; Reginensi et al., 2011; Seymour et al., 2012; Chang et al., 2013; Rockich et al., 2013).

### Roles of Sox9 in lacrimal gland branching morphogenesis

Sox9 expression displayed dynamic changes during early ocular surface development. Sox9 was initially expressed in the lens pit, but subsequently localized to the presumptive conjunctival epithelium and then to the lacrimal and harderian gland epithelia later in fetal life. *Sox9* deletion in the ocular surface epithelium prevented the development of the lacrimal and harderian glands, reduced the number of meibomian glands, but did not alter goblet cell formation. Sox9 and FGF signaling regulated Sox10 expression, which is required for the formation of secretory acinar structures. Sox9 and FGF signaling co-regulated ECM production during the formation and elongation of the lacrimal gland. FGF signaling regulated Sox9 and, in turn, Sox9 may promote FGF signaling though regulating the expression of heparan sulfate-synthesizing enzymes (Fig. 10), although no evidence of a feed-forward loop between Sox9 expression and mesenchymal Fgf10 was detected.

Components of the ECM, including collagens, laminins, glycoproteins and proteoglycans, are essential for branching morphogenesis (Lu et al., 2011; Pritchett et al., 2011; Kim and Nelson, 2012; Daley and Yamada, 2013). Sox9 has been reported to regulate several genes encoding ECM components (Pritchett et al., 2011). In submandibular gland (SMG) branching morphogenesis, the initiation of SMG cleft formation is blocked by collagenase treatment, whereas inhibiting collagenase enhances the number of clefts (Nakanishi et al., 1986; Fukuda et al., 1988). During lung development, Sox9 is required for the expression of the ECM protein Col2a1 (Rockich et al., 2013). In our data, Mia1, collagen II and IX decreased in $Sox9^{CKO}$ embryos during early lacrimal gland morphogenesis, suggesting that these cartilage-associated proteins might contribute to the formation and elongation of the lacrimal bud.

### Sox10 regulates a unique pathway to promote the formation of secretory acini

Sox10 expression was first detected in the forming lacrimal bud and remained localized to the lacrimal bud tip cells along with Mia1, which is also expressed in the tips of lung buds in an FGF-dependent manner (Lin et al., 2008). Lacrimal bud formation was inhibited in *Sox10* conditional knockouts, even though Sox9 expression persisted. In the absence of *Sox10*, lacrimal buds elongated slowly and failed to form lobes and acini. However, transcripts regulated by Sox9 were not affected by *Sox10* deletion, suggesting that Sox9 and Sox10 regulate separate pathways in the lacrimal gland. Identifying the Sox10-specific pathways in the lacrimal buds will require additional experiments.

Development (2014) 141, 2691-2701 doi:10.1242/dev.108944

**Table 2. Lacrimal gland phenotype of *Sox9*$^{+/Het}$ mice is moderately affected by overexpressing a constitutively active FGF receptor**

| | Lacrimal gland phenotype (%) | | | | |
|---|---|---|---|---|---|
| Genotype | Normal | Small branches | Exorbital lobe absent | Absent | *n* |
| *Sox9*$^{+/+}$; *TRE-Fgfr1*$^{-}$ | 11 (91.67) | 0 (0) | 1 (8.33) | 0 (0) | 12 |
| *Sox9*$^{+/+}$; *TRE-Fgfr1*$^{+}$ | 10 (100) | 0 (0) | 0 (0) | 0 (0) | 10 |
| *Sox9*$^{Het}$; *TRE-Fgfr1*$^{-}$ | 1 (2.08) | 1 (2.08) | 32 (66.67) | 14 (29.17) | 48 |
| *Sox9*$^{Het}$; *TRE-Fgfr1*$^{+}$ | 2 (4.35) | 0 (0) | 41 (89.13) | 3 (6.52) | 46 |

Activation of epithelial FGF signaling increased the number of mice with lacrimal glands, but the percentage lacking an exorbital lobe also increased.
*n*, number of lacrimal glands examined.

### FGF signaling and Sox9 function together to promote Sox10 expression

FGF signaling is crucial for the development of the lacrimal gland. Deletion of the ligand Fgf10, the receptor Fgfr2, or the heparin- and GAG-synthesizing enzymes (Ugdh, Ndst1, Ndst2, Hs2st and Hs6st) each block or cause severe defects in lacrimal gland differentiation (Makarenkova et al., 2000; Pan et al., 2008; Qu et al., 2011, 2012). Epithelial deletion of *Fgfr2* decreased Sox9 expression and eliminated Sox10 expression. The persistence of Sox9 in the absence of FGF signaling suggests that Sox9 expression might be regulated by other signaling pathways that contribute to lacrimal gland morphogenesis. This raises the possibility that FGF signaling functions together with Sox9 to control the expression of Sox10.

The expression of Sox9 and of Sox10 are dependent on FGF signaling in other tissues and these SoxE subgroup members often work together during embryogenesis. FGF-coated beads induce the expression of Sox9 and Sox10 to form ectopic neural crest cells from non-neural ectoderm (Yardley and Garcia-Castro, 2012), and the expression of Sox10 in the neural crest is strongly inhibited by an inhibitor of FGF receptor signaling (Honore et al., 2003). The expression of Sox10 is reduced by deletion of *Sox9* in the neural crest (Cheung et al., 2005), and Sox10 protein activates *Sox9* transcription in the gonads of XX mice *in vivo* during sex development (Polanco et al., 2010).

### Sox9 may establish 'baseline' gene expression to promote FGF signaling through the expression of heparin-synthesizing enzymes

Sox9 and Fgf10-Fgfr2 signaling display diverse relationships of regulation. *Fgfr2* deletion leads to decreased Sox9 expression in the distal lung bud epithelium (Abler et al., 2009) and FGFs enhance Sox9 expression through the MAP kinase pathway in chondrogenesis (Abler et al., 2009). During Sertoli cell differentiation and testis development, Fgfr2 is important for the maintenance of Sox9 expression and Sox9 is required for Fgfr2 nuclear localization (Bagheri-Fam et al., 2008). Sox9 and Fgf10-Fgfr2b form a feed-forward loop in the pancreatic progenitor cell niche that maintains pancreatic organ identity. Fgf10-Fgfr2 signaling maintains Sox9 expression in progenitors. In turn, Sox9 is required for Fgfr2b expression and receptivity to Fgf10 (Seymour et al., 2012). A specific MEK inhibitor, which blocks the phosphorylation of Erk1 and Erk2 (Mapk3 and Mapk1), inhibits the increase in Sox9 levels induced by FGFs. Sox9 also functions downstream of FGF/K-ras to promote branching during lung development (Chang et al., 2013).

Our data showed that FGF signaling regulates the expression of Sox9, but that *Sox9* deletion does not affect the expression of *Fgfr2* in the conjunctival epithelium or of *Fgf10* in the adjacent mesenchyme. However, the expression of several FGF downstream response genes was reduced after *Sox9* deletion (Fig. 8). This led us to examine how Sox9 might regulate FGF signaling. It is known that heparan sulfate is required for FGF-FGFR interaction. Inactivation of heparin-synthesizing enzymes disrupts FGF signaling and prevents lacrimal gland formation. However, the mechanism by which the heparin-synthesizing enzymes are regulated remains unclear. It has been demonstrated that heparan sulfate modification depends on functional Fgfr2 and Shp2 (Ptpn11) in the lacrimal gland primordium (Pan et al., 2008, 2010). These studies suggest that feedback is established between heparan sulfation and FGF signaling for the proper regulation of lacrimal gland branching morphogenesis. Our data showed that Sox9 is required for full expression of a subset of heparin-synthesizing enzymes (Hs3st3b1 and Hs3st3a1) in the lacrimal bud epithelium. This suggests that Sox9 might promote FGF signaling by enhancing the synthesis of heparan sulfate and other ECM components, which are required for the FGF-FGFR interaction.

However, increasing FGF signaling by overexpressing a constitutively active form of Fgfr1 only partly restored lacrimal gland defects in *Sox9* heterozygotes. These mice were missing fewer lacrimal glands, but a greater percentage of glands lacked the exorbital lobe or exhibited a vestigial exorbital lobe. This might be explained if most of the lacrimal glands gained by activation of FGF signaling failed to form an exorbital lobe. Although it is possible that Fgfr1 signals differently from Fgfr2, expression of constitutively active Fgfr1 increased ERK signaling to a similar degree as wild-type Fgfr2. These results suggest that Sox9 plays a crucial, largely FGF-independent role in regulating lacrimal gland formation.

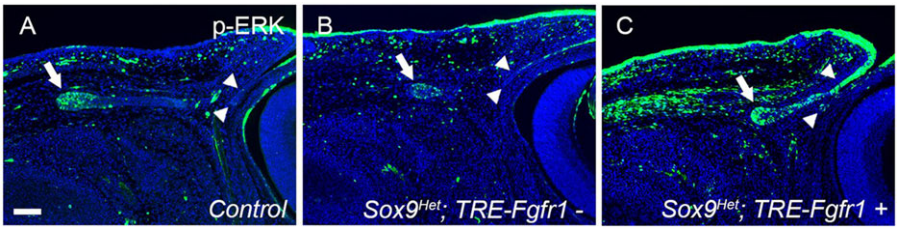


**Fig. 9. Increased FGF signaling in the ocular surface epithelium moderately improves lacrimal gland defects in *Sox9*$^{Het}$ eyes.** Activation of FGF signaling in the ocular surface epithelium increases the levels of phospho-ERK at E15.5. In wild-type (control) mice, phosphorylation of ERK was apparent in the lacrimal bud tip (A, arrow) and was decreased in *Sox9*$^{Het}$; *TRE-Fgfr1*$^{-}$ mice (B, arrow). However, phospho-ERK was not detected in the conjunctival epithelium of control (A, arrowheads) or *Sox9*$^{Het}$; *TRE-Fgfr1*$^{-}$ (B, arrowheads) mice. In *Sox9*$^{Het}$; *TRE-Fgfr1*$^{+}$ mice, ERK was intensely phosphorylated in the lacrimal bud and conjunctival epithelium (C, arrow and arrowheads), compared with the control and with *Sox9*$^{Het}$; *TRE-Fgfr1*$^{-}$ mice. Scale bar: 100 μm.

Development (2014) 141, 2691-2701 doi:10.1242/dev.108944

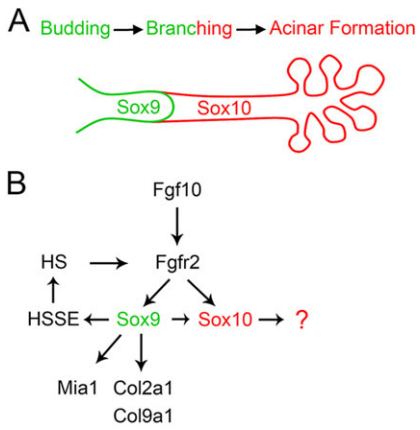


**Fig. 10. Model of Sox9, Sox10 and FGF function during lacrimal gland branching morphogenesis.** (A) Sox9 controls the initial budding and the elongation of the lacrimal bud; Sox10 is activated by Sox9 and continues the elongation and branching of the lacrimal bud and controls the formation of secretory acini. (B) Fgf10 regulates the expression of Sox9 and Sox10. In turn, Sox9 regulates the expression of heparan sulfate-synthesizing enzymes (HSSE), which are required for the synthesis and function of heparan sulfate (HS), to promote FGF signaling. Sox9 and FGF signaling regulate ECM components, which may contribute to the formation and elongation of the lacrimal bud. Identifying the Sox10-specific pathways in the lacrimal buds will require further exploration.

Additional investigations are needed to fully understand the functions of Sox9 and Sox10 in lacrimal gland formation. However, $Sox9^{CKO}$ mice, with their defects in lacrimal, harderian and meibomian glands, might provide a useful model to test therapies for conditions such as severe dry eye disease.

## MATERIALS AND METHODS

### Mice and doxycycline administration

*Sox9* floxed mice were obtained from the Jackson Laboratory (stock number 013106). *Le-Cre* and *Fgfr2* floxed mice have been described previously (Ashery-Padan et al., 2000; Yu et al., 2003; Huang et al., 2009). *Sox10* floxed mice were kindly provided by Drs Michael Wegner and Bill Pavan (Finzsch et al., 2010). *Rosa26-rtTA; TRE-Fgfr1* mice were kindly provided by Drs David Ornitz, Sung-Ho Huh and Kory Lavine (Belteki et al., 2005; Cilvik et al., 2013). Mating mice that were homozygous or heterozygous for the floxed allele, only one of which was Cre positive, resulted in litters in which about half of the offspring were Cre positive. Unless otherwise stated, animals that were Cre positive but lacked a floxed allele (wild type) were used as controls. Noon of the day when the vaginal plug was detected was considered E0.5. Embryos were collected at the desired stages ($n$=3-5 for each genotype and stage).

To activate the *Rosa26-rtTA; TRE-Fgfr1* transgene, the *Le-Cre* transgene was expressed in the ocular surface epithelium to remove a STOP sequence upstream of *Rosa26-rtTA*, and doxycycline was administered in the food (200 mg/kg; Bio-Serv, S3888) beginning at E11.5 until the time of sacrifice. Experiments were approved by the Washington University Animal Studies Committee and conformed to ARVO guidelines for the use of animals in research.

### Histology

Embryo heads were fixed in 4% paraformaldehyde in PBS overnight at 4°C and processed by paraffin embedding and sectioning using conventional methods. For morphological studies, sections were deparaffinized and stained with H&E (Surgipath) or the Accustain periodic acid-Schiff (PAS) kit (Sigma).

### FISH on paraffin sections and cryosections

FISH was performed on paraffin and frozen sections using the Quantigene ViewRNA *in situ* hybridization tissue assay (Affymetrix) according to the manufacturer's instructions. For paraffin sections, FISH conditions were optimized to include a 5 min boiling and 5 min protease (Protease QF, Affymetrix Quantigene ISH kit, QVT0050; 1:200) treatment. For cryosections, 5 min protease (Protease QF, 1:200) treatment was used. Oligonucleotide probes (Type 1 probe set) were designed by Affymetrix (RefSeq RNA ID, Affymetrix probe ID): mouse *Mia1* (NM_019394, VB1-14712), *Fgf10* (NM_008002, VB1-13839), *Hs3st3b1* (NM_018805, VB1-15256) and *Etv5* (NM_023794, VB1-10565) for paraffin sections and *Krt4* (NM_008475, VB1-13838) and *Hs3st3a1* (NM_178870, VB1-15255) for cryosections.

### Immunohistochemical staining

Deparaffinized slides were treated with 3% $H_2O_2$ in PBS to inactivate endogenous peroxidase activity. Antigen retrieval was performed in 0.01 M citrate buffer (pH 6.0) by placing the slides in a pressure cooker for 5 min. After cooling, sections were blocked with 5% goat serum/3% BSA/0.1% Triton X-100 in PBS at room temperature for 1 h and incubated with primary antibody at 4°C overnight, followed by incubation in biotinylated secondary antibodies for 1 h at room temperature and ABC reagent from the Vectastain Elite ABC Kit (Vector Laboratories) for 30 min. Finally, sections were processed with Tyramide Signal Amplification (TSA) Systems (PerkinElmer) for detection. The rabbit anti-Sox9 (sc-20095; 1:100), mouse anti-Sox10 (sc-365692; 1:100) and rabbit anti-Col9a1 (sc-134753; 1:100) antibodies were from Santa Cruz Biotechnology. The rabbit phospho-ERK1/2 antibody was from Cell Signaling Technology (#4370; 1:100). The rabbit Col2a1 antibody was from Abcam (ab34712; 1:100).

### Laser microdissection, microarray analysis and qPCR analysis

Laser microdissection was performed as described previously (Huang et al., 2011). Briefly, E14.5 embryos were embedded in OCT compound (Sakura Finetek) and snap frozen on dry ice. Frozen sections (12 µm) were transferred to glass PEN foil slides (Leica Microsystems, #11505189). Slides were dipped in 70% ethanol at 4°C for 1 min, washed in RNase-free water twice for 30 s each, rinsed in 95% ethanol, and stained in Eosin Y (Sigma). Stained samples were washed in 95% ethanol, dehydrated in 100% ethanol and dried.

To identify differentially expressed transcripts in the *Sox9* conditional knockouts, one sample from wild-type and knockout embryos was dissected from the dorsal, nasal and temporal conjunctival epithelia using a Leica LMD 6000 laser microdissection system. For the *Fgfr2* conditional knockouts, fornical conjunctival epithelium was laser microdissected from three wild-type and three conditional knockout embryos. Approximately 30 ng of total RNA was extracted from the tissue using the RNeasy Microkit (Qiagen, #74004); 10 ng total RNA was reverse transcribed and amplified to produce 3-5 µg cDNA using the WT-Ovation Pico RNA Amplification System (NuGEN Technologies, #3302). The amplified cDNA samples were used for the microarray and qPCR analyses. The $Sox9^{CKO}$ microarrays (Illumina Mouse-6 beadchip) were used to identify transcripts that were selectively expressed in the temporal conjunctiva of wild-type embryos and expressed at reduced levels in knockout embryos. Differentially expressed transcripts were confirmed by qPCR and FISH. For the $Fgfr2^{CKO}$ microarrays, triplicate samples of wild-type and knockout conjunctival epithelia were used to probe Illumina Mouse-6 beadchip microarrays. Microarray data were analyzed using Illumina Genome Studio software. Microarray data are available at Gene Expression Omnibus under combined accession GSE54802.

The qPCR analysis was performed using SYBR Green JumpStart Taq ReadyMix (s4438, Sigma) and the Eco Real-Time PCR System (Illumina) according to the manufacturers' protocols. Quantified values for each gene of interest were normalized against the input determined by the housekeeping gene beta-actin (*Actb*, NM_007393). Primer pairs are listed in supplementary material Table S1. The melting temperature for the *Fgfr2*, *Etv5*, *Dusp6*, *Spry2*, *Hs3st3b1*, *Hs3st3a1*, *Hs2st1*, *Hs6st1* and *Hs6st2* primers was 55°C, and for the *Sox9* and *Sox10* primers 59°C. Each assay was performed in triplicate. For all qPCR experiments, three independent biological samples were analyzed. Statistical analysis was performed using Student's $t$-test. Results were considered statistically significant at $P<0.05$ (Livak and Schmittgen, 2001).

Development (2014) 141, 2691-2701 doi:10.1242/dev.108944

## Imaging

Brightfield and fluorescent images were taken using a Leica Macrofluor macroscope, Olympus BX60 and BX51 microscopes and a Spot Diagnostic Instruments camera.

### Acknowledgements

We thank Drs Michael Wegner, Bill Pavan, Kory Lavine, Peter Gruss and Ruth Ashery-Padan for generating and providing *Sox10*$^{flox/flox}$, *Fgfr2*$^{flox/flox}$, *Rosa26-rtTA; TRE-Fgfr1* and *Le-Cre* mice; Belinda Dana for preparing the histological sections; and Dr Fang Bai for assistance with statistical analysis.

### Competing interests

The authors declare no competing financial interests.

### Author contributions

Z.C. (co-first author) developed the concepts and approach, performed experiments and analyzed the data and prepared the manuscript prior to submission. J.H. (co-first author) developed the concepts and approach, performed experiments and analyzed the data. Y.L. performed experiments and analyzed the data. L.K.D. performed experiments. S.-H.H. developed the approach. D.O. developed the approach. D.C.B. developed the approach, analyzed the data and prepared the manuscript prior to submission.

### Funding

Research was supported by National Institutes of Health (NIH) grants [EY04853 and EY022643 to D.C.B.], an NIH Core Grant [P30 EY02687] and an unrestricted grant from Research to Prevent Blindness to the Department of Ophthalmology and Visual Sciences. Partial support to the Genome Technologies Access Center for microarray analysis was provided by a NIH Clinical and Translational Science Award to Washington University [UL1 TR000448]. Deposited in PMC for release after 12 months.

### Supplementary material

Supplementary material available online at
http://dev.biologists.org/lookup/suppl/doi:10.1242/dev.108944/-/DC1

### References

**Abler, L. L., Mansour, S. L. and Sun, X.** (2009). Conditional gene inactivation reveals roles for Fgf10 and Fgfr2 in establishing a normal pattern of epithelial branching in the mouse lung. *Dev. Dyn.* **238**, 1999-2013.

**Akiyama, H., Chaboissier, M.-C., Martin, J. F., Schedl, A. and de Crombrugghe, B.** (2002). The transcription factor Sox9 has essential roles in successive steps of the chondrocyte differentiation pathway and is required for expression of Sox5 and Sox6. *Genes Dev.* **16**, 2813-2828.

**Ashery-Padan, R., Marquardt, T., Zhou, X. and Gruss, P.** (2000). Pax6 activity in the lens primordium is required for lens formation and for correct placement of a single retina in the eye. *Genes Dev.* **14**, 2701-2711.

**Bagheri-Fam, S., Sim, H., Bernard, P., Jayakody, I., Taketo, M. M., Scherer, G. and Harley, V. R.** (2008). Loss of Fgfr2 leads to partial XY sex reversal. *Dev. Biol.* **314**, 71-83.

**Belteki, G., Haigh, J., Kabacs, N., Haigh, K., Sison, K., Costantini, F., Whitsett, J., Quaggin, S. E. and Nagy, A.** (2005). Conditional and inducible transgene expression in mice through the combinatorial use of Cre-mediated recombination and tetracycline induction. *Nucleic Acids Res.* **33**, e51.

**Bridgewater, L. C., Lefebvre, V. and de Crombrugghe, B.** (1998). Chondrocyte-specific enhancer elements in the Col11a2 gene resemble the Col2a1 tissue-specific enhancer. *J. Biol. Chem.* **273**, 14998-15006.

**Chang, D. R., Martinez Alanis, D., Miller, R. K., Ji, H., Akiyama, H., McCrea, P. D. and Chen, J.** (2013). Lung epithelial branching program antagonizes alveolar differentiation. *Proc. Natl. Acad. Sci. U.S.A.* **110**, 18042-18051.

**Cheung, M., Chaboissier, M.-C., Mynett, A., Hirst, E., Schedl, A. and Briscoe, J.** (2005). The transcriptional control of trunk neural crest induction, survival, and delamination. *Dev. Cell* **8**, 179-192.

**Cilvik, S. N., Wang, J. I., Lavine, K. J., Uchida, K., Castro, A., Gierasch, C. M., Weinheimer, C. J., House, S. L., Kovacs, A., Nichols, C. G. et al.** (2013). Fibroblast growth factor receptor 1 signaling in adult cardiomyocytes increases contractility and results in a hypertrophic cardiomyopathy. *PLoS ONE* **8**, e82979.

**Daley, W. P. and Yamada, K. M.** (2013). ECM-modulated cellular dynamics as a driving force for tissue morphogenesis. *Curr. Opin. Genet. Dev.* **23**, 408-414.

**Dean, C., Ito, M., Makarenkova, H. P., Faber, S. C. and Lang, R. A.** (2004). Bmp7 regulates branching morphogenesis of the lacrimal gland by promoting mesenchymal proliferation and condensation. *Development* **131**, 4155-4165.

**Finzsch, M., Schreiner, S., Kichko, T., Reeh, P., Tamm, E. R., Bosl, M. R., Meijer, D. and Wegner, M.** (2010). Sox10 is required for Schwann cell identity and progression beyond the immature Schwann cell stage. *J. Cell Biol.* **189**, 701-712.

**Foster, J. W., Dominguez-Steglich, M. A., Guioli, S., Kwok, C., Weller, P. A., Stevanović, M., Weissenbach, J., Mansour, S., Young, I. D., Goodfellow, P. N. et al.** (1994). Campomelic dysplasia and autosomal sex reversal caused by mutations in an SRY-related gene. *Nature* **372**, 525-530.

**Fukuda, Y., Masuda, Y., Kishi, J., Hashimoto, Y., Hayakawa, T., Nogawa, H. and Nakanishi, Y.** (1988). The role of interstitial collagens in cleft formation of mouse embryonic submandibular gland during initial branching. *Development* **103**, 259-267.

**Furuyama, K., Kawaguchi, Y., Akiyama, H., Horiguchi, M., Kodama, S., Kuhara, T., Hosokawa, S., Elbahrawy, A., Soeda, T., Koizumi, M. et al.** (2011). Continuous cell supply from a Sox9-expressing progenitor zone in adult liver, exocrine pancreas and intestine. *Nat. Genet.* **43**, 34-41.

**Govindarajan, V., Ito, M., Makarenkova, H. P., Lang, R. A. and Overbeek, P. A.** (2000). Endogenous and ectopic gland induction by FGF-10. *Dev. Biol.* **225**, 188-200.

**Honoré, S. M., Aybar, M. J. and Mayor, R.** (2003). Sox10 is required for the early development of the prospective neural crest in Xenopus embryos. *Dev. Biol.* **260**, 79-96.

**Huang, J., Dattilo, L. K., Rajagopal, R., Liu, Y., Kaartinen, V., Mishina, Y., Deng, C.-X., Umans, L., Zwijsen, A., Roberts, A. B. et al.** (2009). FGF-regulated BMP signaling is required for eyelid closure and to specify conjunctival epithelial cell fate. *Development* **136**, 1741-1750.

**Huang, J., Rajagopal, R., Liu, Y., Dattilo, L. K., Shaham, O., Ashery-Padan, R. and Beebe, D. C.** (2011). The mechanism of lens placode formation: a case of matrix-mediated morphogenesis. *Dev. Biol.* **355**, 32-42.

**Kenchegowda, D., Swamynathan, S., Gupta, D., Wan, H., Whitsett, J. and Swamynathan, S. K.** (2011). Conditional disruption of mouse Klf5 results in defective eyelids with malformed meibomian glands, abnormal cornea and loss of conjunctival goblet cells. *Dev. Biol.* **356**, 5-18.

**Kim, H. Y. and Nelson, C. M.** (2012). Extracellular matrix and cytoskeletal dynamics during branching morphogenesis. *Organogenesis* **8**, 56-64.

**Laclef, C., Souil, E., Demignon, J. and Maire, P.** (2003). Thymus, kidney and craniofacial abnormalities in Six1 deficient mice. *Mech. Dev.* **120**, 669-679.

**Lin, S., Ikegami, M., Xu, Y., Bosserhoff, A.-K., Malkinson, A. M. and Shannon, J. M.** (2008). Misexpression of MIA disrupts lung morphogenesis and causes neonatal death. *Dev. Biol.* **316**, 441-455.

**Livak, K. J. and Schmittgen, T. D.** (2001). Analysis of relative gene expression data using real-time quantitative PCR and the 2(-Delta Delta C(T)) Method. *Methods* **25**, 402-408.

**Lu, P., Takai, K., Weaver, V. M. and Werb, Z.** (2011). Extracellular matrix degradation and remodeling in development and disease. *Cold Spring Harb. Perspect. Biol.* **3**, a005058.

**Makarenkova, H. P., Ito, M., Govindarajan, V., Faber, S. C., Sun, L., McMahon, G., Overbeek, P. A. and Lang, R. A.** (2000). FGF10 is an inducer and Pax6 a competence factor for lacrimal gland development. *Development* **127**, 2563-2572.

**Mattiske, D., Sommer, P., Kidson, S. H. and Hogan, B. L. M.** (2006). The role of the forkhead transcription factor, Foxc1, in the development of the mouse lacrimal gland. *Dev. Dyn.* **235**, 1074-1080.

**Nakanishi, Y., Sugiura, F., Kishi, J.-I. and Hayakawa, T.** (1986). Collagenase inhibitor stimulates cleft formation during early morphogenesis of mouse salivary gland. *Dev. Biol.* **113**, 201-206.

**Pan, Y., Carbe, C., Powers, A., Zhang, E. E., Esko, J. D., Grobe, K., Feng, G.-S. and Zhang, X.** (2008). Bud specific N-sulfation of heparan sulfate regulates Shp2-dependent FGF signaling during lacrimal gland induction. *Development* **135**, 301-310.

**Pan, Y., Carbe, C., Powers, A., Feng, G.-S. and Zhang, X.** (2010). Sprouty2-modulated Kras signaling rescues Shp2 deficiency during lens and lacrimal gland development. *Development* **137**, 1085-1093.

**Polanco, J. C., Wilhelm, D., Davidson, T.-L., Knight, D. and Koopman, P.** (2010). Sox10 gain-of-function causes XX sex reversal in mice: implications for human 22q-linked disorders of sex development. *Hum. Mol. Genet.* **19**, 506-516.

**Pritchett, J., Athwal, V., Roberts, N., Hanley, N. A. and Hanley, K. P.** (2011). Understanding the role of SOX9 in acquired diseases: lessons from development. *Trends Mol. Med.* **17**, 166-174.

**Qu, X., Carbe, C., Tao, C., Powers, A., Lawrence, R., van Kuppevelt, T. H., Cardoso, W. V., Grobe, K., Esko, J. D. and Zhang, X.** (2011). Lacrimal gland development and Fgf10-Fgfr2b signaling are controlled by 2-O- and 6-O-sulfated heparan sulfate. *J. Biol. Chem.* **286**, 14435-14444.

**Qu, X., Pan, Y., Carbe, C., Powers, A., Grobe, K. and Zhang, X.** (2012). Glycosaminoglycan-dependent restriction of FGF diffusion is necessary for lacrimal gland development. *Development* **139**, 2730-2739.

**Reginensi, A., Clarkson, M., Neirijnck, Y., Lu, B., Ohyama, T., Groves, A. K., Sock, E., Wegner, M., Costantini, F., Chaboissier, M.-C. et al.** (2011). SOX9 controls epithelial branching by activating RET effector genes during kidney development. *Hum. Mol. Genet.* **20**, 1143-1153.

**Rockich, B. E., Hrycaj, S. M., Shih, H. P., Nagy, M. S., Ferguson, M. A. H., Kopp, J. L., Sander, M., Wellik, D. M. and Spence, J. R.** (2013). Sox9 plays multiple roles in the lung epithelium during branching morphogenesis. *Proc. Natl. Acad. Sci. U.S.A.* **110**, E4456-E4464.

**Schubert, T., Schlegel, J., Schmid, R., Opolka, A., Grässel, S., Humphries, M. and Bosserhoff, A.-K.** (2010). Modulation of cartilage differentiation by

Development (2014) 141, 2691-2701 doi:10.1242/dev.108944

melanoma inhibiting activity/cartilage-derived retinoic acid-sensitive protein (MIA/CD-RAP). *Exp. Mol. Med.* **42**, 166-174.

**Seymour, P. A., Shih, H. P., Patel, N. A., Freude, K. K., Xie, R., Lim, C. J. and Sander, M.** (2012). A Sox9/Fgf feed-forward loop maintains pancreatic organ identity. *Development* **139**, 3363-3372.

**Tsau, C., Ito, M., Gromova, A., Hoffman, M. P., Meech, R. and Makarenkova, H. P.** (2011). Barx2 and Fgf10 regulate ocular glands branching morphogenesis by controlling extracellular matrix remodeling. *Development* **138**, 3307-3317.

**Vidal, V. P. I., Chaboissier, M.-C., Lützkendorf, S., Cotsarelis, G., Mill, P., Hui, C.-C., Ortonne, N., Ortonne, J.-P. and Schedl, A.** (2005). Sox9 is essential for outer root sheath differentiation and the formation of the hair stem cell compartment. *Curr. Biol.* **15**, 1340-1351.

**Xie, W.-F., Zhang, X., Sakano, S., Lefebvre, V. and Sandell, L. J.** (1999). Trans-activation of the mouse cartilage-derived retinoic acid-sensitive protein gene by Sox9. *J. Bone Miner. Res.* **14**, 757-763.

**Yardley, N. and García-Castro, M. I.** (2012). FGF signaling transforms non-neural ectoderm into neural crest. *Dev. Biol.* **372**, 166-177.

**Yu, K., Xu, J., Liu, Z., Sosic, D., Shao, J., Olson, E. N., Towler, D. A. and Ornitz, D. M.** (2003). Conditional inactivation of FGF receptor 2 reveals an essential role for FGF signaling in the regulation of osteoblast function and bone growth. *Development* **130**, 3063-3074.